

# Photon channel perspective on high harmonic generation

Liang Li,<sup>1</sup> Xiaosong Zhu,<sup>1</sup> Pengfei Lan,<sup>1,\*</sup> Lixin He,<sup>1</sup>, and Peixiang Lu<sup>1,2†</sup>

<sup>1</sup>*School of Physics and Wuhan National Laboratory for Optoelectronics,  
Huazhong University of Science and Technology, Wuhan 430074, China*

<sup>2</sup>*Laboratory of Optical Information Technology,  
Wuhan Institute of Technology, Wuhan 430205, China*

(Dated: June 7, 2019)

## Abstract

A photon channel perspective on high harmonic generation (HHG) is proposed by using a non-perturbative full quantum theory. It is shown that the HHG yield can be expressed as a sum of the contribution of all the photon channels. From this perspective, the contribution of a specific photon channel follows a brief analytical formula and the competition between the channels is well interpreted. Our prediction is shown to be in good agreement with the simulations with time-dependent Schrödinger equation. It also recovers the perturbative interpretation of the HHG in a noncollinear two-color field.

---

\* pengfeilan@hust.edu.cn

† lupeixiang@hust.edu.cn

High harmonic generation (HHG) is a highly nonlinear process in the interaction between the atom (or molecule) and the intense laser field. The HHG spectrum has a general characteristic: it falls off for the first few harmonics, then exhibits a broad plateau where all the harmonics have the comparable intensity and ends up with a sharp cutoff. Single or trains of attosecond pulses can be generated by coherently synthesizing a series of high harmonics [1–4], which enables us to steer and probe the nuclear and electronic dynamics in an unprecedentedly fast time scale [5–7]. By using a semiclassical approach, the three-step model (TSM) has been established [8, 9], which gives a very clear physical picture of HHG. According to this model, the electron tunnel ionized from the ground state into the continuum is classically driven by the laser field and the high harmonics are emitted by the recollision process.

There are many theoretical methods developed to investigate the HHG. By numerically solving the time-dependent Schrödinger equation (TDSE), one can well reproduce the HHG. Nevertheless, the rich information is encoded in the electronic wave function. It is not straightforward to reveal the underlying physics. Therefore, many other approaches such as the Lewenstein model [10], the quantum orbits (QO) theory [11–13], quantitatively rescattering (QRS) theory [14–16] and factorization methods [17, 18] have been developed. With these theories, the HHG process can be quantitatively illustrated in terms of the electron trajectories (or quantum orbits [11]) driven by the laser field similar to TSM. Lots of experimental observations can be well interpreted, e.g., the cut-off law and the long or short trajectory.

All the theories mentioned above treat the laser field and the generated high harmonics as waves. It gives a good description of HHG within the wave picture, but fails to explain the photon-like quantum properties of HHG. As is known, wave-particle duality is the elementary nature of the driving laser and high harmonics. However, the theory of HHG within photon picture is scarce [19, 20]. Recently, HHG in the noncollinear two-color laser field [21, 22] and non-pure vortex beam [23] are drawing increasing attention in both fundamental studies and applications. To explain the complex features of the generated high harmonics, the concept of photon channel was employed. With this concept, one can intuitively understand the HHG in terms of absorbing and emitting specific numbers of photons required by the selection rules or conservation laws [21–24]. However, the photon channel is only phenomenologically applied. The HHG theory from photon channel perspective is far from being quantitatively

formulated and the underlying physics of the photon channel is still not well understood. In this case, it creates demands for establishing a theoretical representation of HHG in the frame of photon picture.

In this Letter, we propose a photon channel perspective on HHG in the two-color field by utilizing a non-perturbative quantum theory, where both the laser field and high harmonics are treated as photons. By analogy with the path integration, the HHG emission amplitude can be expressed in terms of the quantum paths. The sum of the quantum paths with the same number of photons  $n_1$  and  $n_2$  absorbed from each driving fields is defined as a photon channel. It is shown that although the HHG driven by non-pure field has complicated features, the contribution of a specific photon channel follows a brief analytical formula. The photon channel competition and the scaling law of HHG yield can be well interpreted in terms of this formula.

To illustrate our model, we consider the HHG in a two-color field. The laser intensities, frequencies and wave vectors are denoted by  $I_1$ ,  $I_2$ ,  $\omega_1$ ,  $\omega_2$  and  $k_1$ ,  $k_2$ , respectively. The frequency and wave vector of the emitted high harmonics are denoted by  $\Omega$  and  $k'$ , respectively. Both the two-color laser field and the high harmonics are quantized. Vacuum polarization and other relativistic effects for the electron are ignored. The Hamiltonian of this atom-radiation system is:

$$H = H_0 + H_p + V_L \quad (1)$$

where  $H_0 = \sum_k E_k |k\rangle\langle k|$  and  $H_p = \omega_1 N_1 + \omega_2 N_2 + \Omega N_\Omega$  are Hamiltonian of the field-free atom and photon, respectively.  $E_k$  and  $|k\rangle$  are the eigenenergies and eigenstates of the field-free Hamiltonian of atom ( $E_k < 0$  for bound states and  $E_k > 0$  for continuum states).  $N_1 = (a_1^\dagger a_1 + a_1 a_1^\dagger)/2$ ,  $N_2 = (a_2^\dagger a_2 + a_2 a_2^\dagger)/2$ ,  $N_\Omega = ((a')^\dagger a' + a'(a')^\dagger)/2$  are the photon number operators of the laser and the harmonic photon mode, respectively.  $a$  and  $a^\dagger$  are the annihilation and creation operators.  $V_L = -\mathbf{d} \cdot (\mathbf{E}_1 + \mathbf{E}_2 + \mathbf{E}')$  is the electron-photon interaction, where  $\mathbf{d} = \sum_j |j\rangle\langle j| \mathbf{d} \sum_k |k\rangle\langle k| = \sum_{j,k} \mathbf{d}_{jk} |j\rangle\langle k|$  is the dipole moment. The electric fields  $\mathbf{E}_m$  ( $m = 1, 2$ ) and  $\mathbf{E}'$  for the driving laser and the generated harmonics can be expressed as  $\mathbf{E}_m = ig_m(\hat{\epsilon}_m a_m e^{i\mathbf{k}_m \cdot \mathbf{r}} - c.c.)$  and  $\mathbf{E}' = ig'(\hat{\epsilon}' a' e^{i\mathbf{k}' \cdot \mathbf{r}} - c.c.)$ .  $g_m = (2\omega_m/V)^{1/2}$ ,  $g' = (2\Omega/V')^{1/2}$  where  $V$  and  $V'$  are the normalization volumes of the photon modes.  $\hat{\epsilon}_m = \hat{\epsilon}_x \cos(\theta_m) + i\hat{\epsilon}_y \sin(\theta_m)$  and  $\hat{\epsilon}' = \hat{\epsilon}_x \cos(\theta') + i\hat{\epsilon}_y \sin(\theta')$  are the transverse polarization. The long-wavelength approximation ( $\lambda \gg r_{electron}$ ) is considered in this work, i.e.  $e^{i\mathbf{k}_m \cdot \mathbf{r}} \approx 1$ ,  $e^{i\mathbf{k}' \cdot \mathbf{r}} \approx 1$  and the electric field is independent of  $r$ .

To clarify the interaction between the atom and the photons, the Hamiltonian is rewritten in Interaction picture

$$\begin{aligned}
H_I(t) &= -\mathbf{D}(t) \cdot \varepsilon(t) \\
\mathbf{D}(t) &= \sum_{j,k} \mathbf{d}_{jk} e^{i\omega_{jk}t} |j\rangle\langle k| \\
\varepsilon(t) &= i \left( \sum_m g_m \hat{\epsilon}_m a_m e^{-i\omega_m t} + g' \hat{\epsilon}' a' e^{-i\Omega t} - c.c \right)
\end{aligned} \tag{2}$$

where  $\omega_{jk} = E_j - E_k$ . We denote the eigenstates of the Hamiltonian  $H_0 + H_p$  as  $|\Psi_{i,j}\rangle$ . We have  $(H_0 + H_p)|\Psi_{i,j}\rangle = E_{i,j}|\Psi_{i,j}\rangle$  with the eigenenergies  $E_{i,j} = E_i + (n_{1j} + 1/2)\omega_1 + (n_{2j} + 1/2)\omega_2 + (n_{\Omega j} + 1/2)\Omega$ . Then, the transition matrix element between the state  $|i\rangle = |\psi\rangle_i$  and  $|f\rangle = |\psi\rangle_f$  is

$$A(i \rightarrow f) = \langle f | e^{-i(H_0 + H_p)t} U_I(t, t_0) | i \rangle, \tag{3}$$

where  $U_I(t, t_0)$  is the time-evolution operator in Interaction picture. Using the Dyson equation,  $U_I$  can be expressed as

$$\begin{aligned}
U_I(t, t_0) &= 1 + \sum_1^\infty U_{In}(t, t_0), \\
U_{In}(t, t_0) &= \left(\frac{1}{i}\right)^n \int_{t_0}^t dt_1 \dots \int_{t_0}^{t_{n-1}} dt_n H_I(t_1) \dots H_I(t_n).
\end{aligned} \tag{4}$$

With Eqs. 3 and 4, the transition matrix element can be rewritten as

$$\begin{aligned}
A(i \rightarrow f) &= \sum A_n(i \rightarrow f), \\
A_n(i \rightarrow f) &= \langle f | e^{-i(H_0 + H_p)t} U_{In}(t, t_0) | i \rangle.
\end{aligned} \tag{5}$$

The initial and final states of HHG are taken as  $|i\rangle = |\phi_0, n_{1i}, n_{2i}, 0\rangle$  and  $|f\rangle = |\phi_0, n_{1f}, n_{2f}, 1\rangle$ , respectively. In this case, we expand  $A_n(i \rightarrow f)$  in terms of  $Qp : (\Omega; \omega^{t_2}, \omega^{t_3}, \dots, \omega^{t_n})$

$$A_n(i \rightarrow f) = e^{-iE_{0f}t} \sum_{Qp} A_n(Qp) \tag{6}$$

where

$$\begin{aligned}
A_n(Qp) &= \left(\frac{1}{i}\right)^n \int_{t_0}^t dt_1 \dots \int_{t_0}^{t_{n-1}} dt_n \langle 1 | a^\dagger e^{-i\Omega t_1} | 0 \rangle \\
&\quad \times \langle n_{1f}, n_{2f} | \varepsilon_{\omega^{t_2}}(t_2) \dots \varepsilon_{\omega^{t_n}}(t_n) | n_{1i}, n_{2i} \rangle \\
&\quad \times \langle \phi_0 | r_1(t_1) \dots r_n(t_n) | \phi_0 \rangle
\end{aligned} \tag{7}$$

$\omega^{t_i}$  denotes the frequency of the photon absorbed at time  $t_i$ . In the two-color field,  $\omega^{t_i} = \omega_1$  or  $\omega_2$ . We define  $Qp : (\Omega; \omega^{t_2}, \omega^{t_3}, \dots, \omega^{t_n})$  as a quantum path, which denotes absorbing a series of photons with frequencies  $\omega^{t_2}, \omega^{t_3}, \dots, \omega^{t_n}$  and emitting a harmonic photon with frequency  $\Omega = \omega^{t_2} + \omega^{t_3} + \dots + \omega^{t_n}$ .  $A_n(Qp)$  describes the transition of the electron-atom system from the initial state  $|i\rangle$  to the final state  $|f\rangle$  via the quantum path  $Qp : (\Omega; \omega^{t_2}, \omega^{t_3}, \dots, \omega^{t_n})$ . Equations 6 and 7 suggest the following perspective on HHG: the probability of emitting a harmonic photon  $\Omega$  can be expressed by summing up the contribution of all the possible quantum paths

$$\begin{aligned}
P(\Omega) &= \rho(\phi_0) |A(i \rightarrow f_\Omega)|^2 \\
&= \rho(\phi_0) \left| \sum_{Qp} A_n(\Omega; \omega^{t_2}, \omega^{t_3}, \dots, \omega^{t_n}) \right|^2 \\
&= \rho(\phi_0) \left| \sum_{Qp} (\sigma_0(Qp) p(\omega^{t_2}) \dots p(\omega^{t_n}))^{1/2} \right|^2.
\end{aligned} \tag{8}$$

Here,  $p(\omega^{t_i}) = p_1$  or  $p_2$  with  $p_m = N_m \omega_m / (N_1 \omega_1 + N_2 \omega_2) = I_m / (I_1 + I_2)$  ( $m = 1$  or  $2$ );  $p_m$  is the corresponding probability for absorbing the  $\omega_m$  photon.  $\rho(\phi_0)$  is the density of the ground state.  $\sigma_0(Qp)$  is the complex amplitude which describes the ability for an atom absorbing a series of photons  $(\Omega; \omega^{t_2}, \omega^{t_3}, \dots, \omega^{t_n})$ . Note that the observation of one high harmonic  $\Omega$  in experiment [21] corresponds to the process that absorbs particular numbers of two-color photons  $(n_1, n_2)$ . This process is contributed by the sum of all the possible quantum paths that can generate the high harmonic  $\Omega = n_1 \omega_1 + n_2 \omega_2$ . We define it as a photon channel  $\Omega(n_1, n_2)$ , where  $n_1$  and  $n_2$  are the number of the absorbed  $\omega_1$  and  $\omega_2$  photons (see Fig. 1).

To validate the above model, we compare the prediction of our formula Eq. 8 against the accurate numerical solutions of TDSE. Note that the photon channels are usually of high degeneracy because the energy conservation equation  $\Omega = n_1 \omega_1 + n_2 \omega_2$  with  $\omega_1 : \omega_2 = 1 : 2$  has multiple solutions [24]. For example, as shown in Fig. 1(a),  $\Omega = 9\omega_1$  can be obtained from the photon channels  $\Omega(9, 0), \Omega(5, 2), \Omega(1, 4)$  and so on. To simplify the analysis, we consider to eliminate the degeneracy by using a two-color field with incommensurate frequencies  $\omega_1 : \omega_2 = 1 : 1.9$  [24]. The linearly polarized 800-nm ( $\omega_1$ ) and 421-nm ( $\omega_2 = 1.9\omega_1$ ) fields are adopted in the simulation and the target atom is hydrogen. We solve the three dimensional TDSE as in [25]. The laser field is turned on linearly over the first 10 optical cycles and is kept constant for another 110 optical cycles. We keep the total intensity

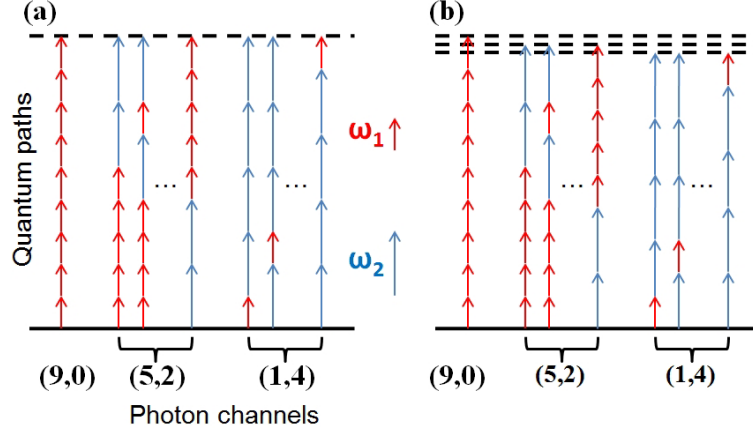


FIG. 1. The sketch of the quantum paths and photon channels of HHG in the two-color field. A photon channel contains many quantum paths as denoted in the brace. (a) Channels for harmonic photon  $\Omega = 9\omega_1$ , where  $\omega_1 : \omega_2 = 1 : 2$ . In this case, the photon channels  $\Omega(9, 0)$ ,  $\Omega(5, 2)$ ,  $\Omega(1, 4)$  are degenerate. (b) Channels for harmonic photon  $\Omega = 9\omega_1, 8.8\omega_1$  and  $8.6\omega_1$ , where  $\omega_1 : \omega_2 = 1 : 1.9$ .

$I = I_1 + I_2$  of the two-color field constant ( $0.2 \times 10^{14} \text{W/cm}^2$ ) and vary  $I_2$ . In this case, we can rewrite Eq. 8 as

$$\begin{aligned}
 P(\Omega) &= \sum_{\Omega=n_1+1.9n_2} P(\Omega(n_1, n_2)) \\
 &= \sum_{\Omega=n_1+1.9n_2} \rho(\phi_0) \sigma(n_1, n_2) p_1^{|n_1|} p_2^{|n_2|}
 \end{aligned} \tag{9}$$

where  $\sigma(n_1, n_2) = |\sum_{Qp} \sigma_0^{1/2}(\Omega; \omega^{t_2}, \omega^{t_3}, \dots, \omega^{t_n})|^2$ . Note that  $|\sigma_0|$  of different quantum paths in a specific photon channel are approximately equal. When the interference of the quantum paths can be ignored,  $\sigma(n_1, n_2) \simeq C_{|n_1|+|n_2|}^{|n_1|} |\sigma_0(\Omega; \omega_1, \omega_1, \dots, \omega_2)|$  (the number of  $\omega_1$  and  $\omega_2$  in the bracket is  $n_1$  and  $n_2$ ). In this case, the contribution of a specific photon channel  $\Omega(n_1, n_2)$  is proportional to  $C_{|n_1|+|n_2|}^{|n_1|} p_1^{|n_1|} p_2^{|n_2|}$ . For  $I_2 \ll I_1$ , the scaling law collapses to the simple form  $I_2^{n_2}$  as the perturbation interpretation [21].

Figure 2 shows the high harmonic spectra obtained with TDSE for different  $p_2$ . The photon channels, e.g.,  $\Omega(15, 0)$ ,  $\Omega(11, 2)$  and  $\Omega(7, 4)$ , can be clearly identified. For a small  $p_2 (= 0.015)$ , the channels with small  $n_2$  are dominant, e.g.  $\Omega(12, 1)$ ,  $\Omega(15, 0)$  and  $\Omega(14, 1)$ . This agrees well with our model (see Eq. 9), because  $p_2^{|n_2|}$  rapidly decreases with increasing  $n_2$ . With increasing  $p_2$ , the multichannel competition becomes obvious and the channels with larger  $n_2$  become dominant. If  $p_2$  is further increased, e.g.,  $p_2 = 0.8$ , the channels with even larger  $n_2$  become dominant. Although the channel competition

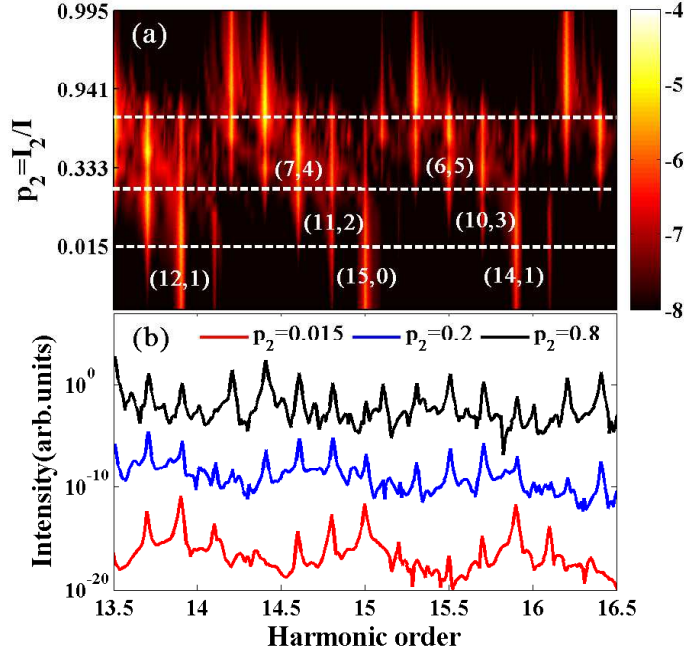


FIG. 2. (a) The HHG spectra for different  $p_2$ . Each channel is labeled as  $(n_1, n_2)$  at frequency  $\Omega = (n_1 + 1.9n_2)\omega_1$ . The colorbar denotes the harmonic yield in logarithmic scale. (b) The HHG spectra for  $p_2 = 0.015, 0.2$  and  $0.8$ . The blue and black curves are shifted vertically by multiplying a factor of  $10^6$  and  $10^{12}$ , respectively.

complicates the high harmonic spectrum, it can be well predicted and explained with Eq. 9. For clarity, we compare the two channels  $\Omega_1(n_1, n_2)$  and  $\Omega_2(n'_1, n'_2)$ , whose ratio  $\gamma(\Omega_1, \Omega_2) = P(\Omega_1(n_1, n_2))/P(\Omega_2(n'_1, n'_2)) \approx C_{|n_1|+|n_2|}^{|n_1|}/C_{|n'_1|+|n'_2|}^{|n'_1|} p_1^{|n_1|-|n'_1|} p_2^{|n_2|-|n'_2|}$ . One can easily obtain that  $\gamma(\Omega(15, 0), \Omega(11, 2)) \approx 80 \gg 1$  at  $p_2 = 0.015$ , i.e., the channel with smaller  $n_2$  is dominant. However,  $\gamma(\Omega_1, \Omega_2)$  quickly decreases as increasing  $p_2$ , e.g.,  $\gamma(\Omega(7, 4), \Omega(3, 6)) \approx 0.01 \ll 1$  at  $p_2 = 0.8$ . The channel with larger  $n_2$  becomes dominant.

Next we discuss the scaling  $p_1^{|n_1|} p_2^{|n_2|}$  of the harmonic yield for a specific photon channel  $\Omega(n_1, n_2)$ . Strictly speaking, the degeneracy of the photon channels cannot be perfectly eliminated in the two-color field with incommensurate frequencies, e.g., the channels  $\Omega(n_1, n_2)$  and  $\Omega'(n_1 - 19, n_2 + 10)$  both satisfy  $\Omega = n_1\omega_1 + 1.9n_2\omega_2$  and contribute to the same harmonic  $\Omega$ . However, because the parameter  $\gamma(\Omega, \Omega') \approx C_{|n_1|+|n_2|}^{|n_1|}/C_{|n_1-19|+|n_2+10|}^{|n_1-19|} p_1^{|n_1|-|n_1-19|} p_2^{|n_2|-|n_2+10|}$  is either  $\ll 1$  or  $\gg 1$  for most values of  $p_2$  and always quickly passes through the point  $\gamma = 1$ , the harmonic  $\Omega$  is usually dominated by one channel. In Fig. 3, we plot, on the log-log scale,

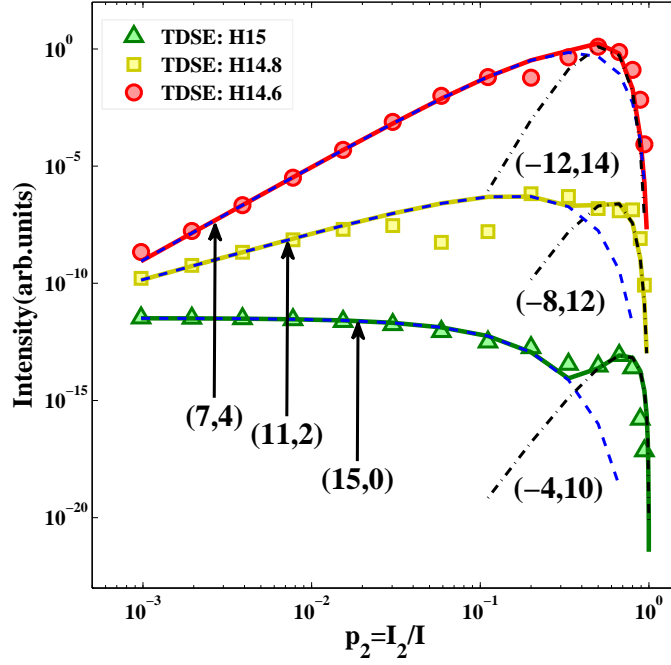


FIG. 3. High harmonic yield as a function of  $p_2$ . The harmonic yield denoted by triangles, squares and circles are obtained with TDSE simulations. The dash and the dash-dot lines show the contributions of different  $(n_1, n_2)$  channels predicted with our model. The solid lines are the sum of them. The laser parameters are same as Fig. 2. Each curve is normalized for clarify.

the high harmonic yield versus  $p_2$ . The triangles, squares and circles show the yields of the harmonics  $15\omega_1$ ,  $14.8\omega_1$  and  $14.6\omega_1$  obtained with TDSE, respectively. The dash and dash-dot lines show the predicted contribution of a specific channel denoted by  $(n_1, n_2)$  with our model, while the solid lines show the sum of two degenerated channels. We first discuss the yield of harmonic  $15\omega_1$ . For a small  $p_2 (< 0.3)$ , our model predicts that the channel  $\Omega(15, 0)$  is dominant and the yield is proportional to  $(1 - p_2)^{15} p_2^0$ . As  $p_2$  becomes larger than 0.3, the dominant channel is converted from  $\Omega(15, 0)$  to  $\Omega(-4, 10)$  and the yield is proportional to  $(1 - p_2)^4 p_2^{10}$ . These scalings and the channel competition are in good accordance with the TDSE simulations. Similar agreements are also found for the other harmonics  $14.8\omega_1$  and  $14.6\omega_1$ . In addition, one sees that the channel competition is more obvious for larger  $n_1$ . This can be well described by the parameter  $\gamma$ . Comparing  $\gamma_1(\Omega(15, 0), \Omega(-4, 10))$  and  $\gamma_2(\Omega(7, 4), \Omega(-12, 14))$ , one can find that  $\gamma_1 \approx C_{15}^0 / C_{14}^4 (1 - p_2)^{11} p_2^{-10}$  decreases monotonically with  $p_2$  and quickly passes through  $\gamma \approx 1$ ; in contrast,  $\gamma_2 \approx C_{11}^4 / C_{26}^{12} (1 - p_2)^{-5} p_2^{-10}$  has



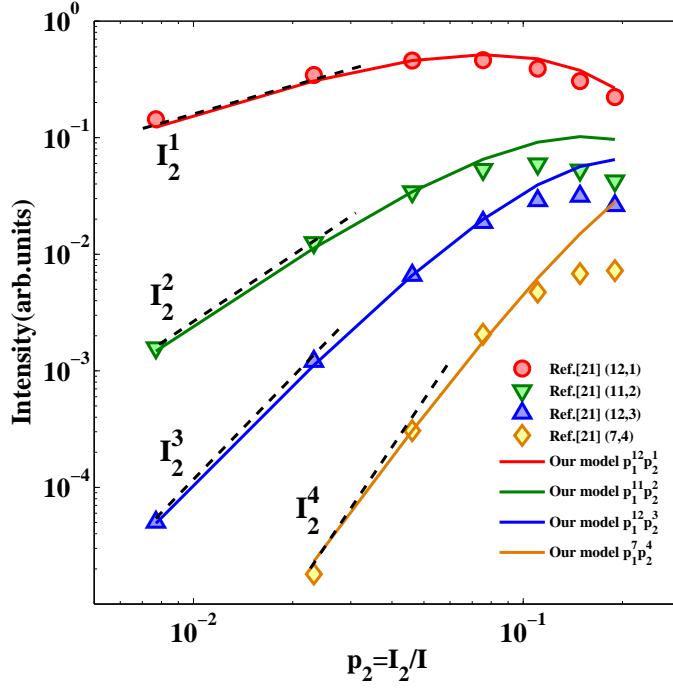


FIG. 4. Comparisons of the predicted HHG yields in the nonlinear two-color field between our model (solid curves) and Ref. [21]. The laser parameters are the same as those in Fig. 3(b) of [21]. Each curve is normalized for comparison.

a minimum and changes slowly near  $\gamma \approx 1$ . Therefore, the conversion of dominant channels is faster and the channel competition is more obvious for channels with larger  $n_1$ .

The derivation of our model is independent of the form of laser field, therefore it can be generalized to other laser fields. To illustrate this, we apply our model to the scenario of a noncollinear two-color field, where the contribution of different photon channels can be well distinguished spatially. We compare our model with the previous work [21]. When  $I_2 \ll I_1 \simeq I$ , the factor  $\rho(\phi_0)\sigma(n_1, n_2)$  in Eq. 9 can be approximated to a constant. As is shown in Fig. 4, for each channels, the harmonic yield first increases, then saturates with increasing  $p_2$  and even decreases with further increasing  $p_2$ . The channel with smaller  $n_2$  saturates at smaller  $p_2$ . In the low intensity region ( $p_2 < 0.04$ ), the yield follows a scaling  $I_2^1$ ,  $I_2^2$  and  $I_2^3$  for the channels  $\Omega(12, 1)$ ,  $\Omega(11, 2)$  and  $\Omega(12, 3)$ , respectively. Our model gives the same results as [21], because the scaling  $p_1^{|n_1|} p_2^{|n_2|}$  collapses to  $I_2^{|n_2|}$  when  $p_2$  approaches to 0. However, the harmonic yield deviates significantly from the scaling law  $I_2^{n_2}$  when  $p_2 > 0.04$ . It becomes saturated near  $p_2 = 0.1$  and even decreases for a higher  $p_2$ . In

contrast, our model still works well when  $p_2 > 0.04$ . Considering the factor  $\rho(\phi_0)\sigma(n_1, n_2)$  is approximately constant, Eq. 9 indicates that the contribution of the channel  $\Omega(n_1, n_2)$  attains its maximum value at  $p_2 = |n_2|/(|n_1| + |n_2|)$ . This well predicts the saturation effect and explain why the process with smaller  $n_2$  saturates earlier. With further increasing the intensity  $I_2$  ( $p_2 > 0.1$ ), the total intensity increases obviously. The factor  $\rho(\phi_0)\sigma(n_1, n_2)$  can not be approximated to constant because of the increasing depletion of the ground state and the variation of  $\sigma(n_1, n_2)$ . Then, the harmonic yield diverges slowly from our prediction. The above results suggest that the HHG in the noncollinear two-color field can be understood essentially from the photon channel perspective. Our model provides a more comprehensive insight of the power scaling law of the HHG yield than the perturbation interpretation [21].

In conclusion, a photon channel perspective of HHG is established based on the non-perturbative quantum theory. We show that HHG can be well understood in terms of photon channels and the photon-like quantum feature of HHG can be investigated by analyzing these photon channels. Our model well explains the channel competition and power scaling law in the two-color field. It also explains the results in the noncollinear case [21] beyond the perturbation region [21]. Such a quantitative model from the photon channel perspective provides a general approach and useful tool for investigating the photon-like features of high harmonics.

This work was supported by the National Natural Science Foundation of China under Grants Nos. 11422435, 11234004 and 11404123.

- 
- [1] G. Farkas and C. Toth, Phys. Lett. A **168**, 447 (1992).
  - [2] I. P. Christov, M.M. Murnane, and H. C. Kapteyn, Phys. Rev. Lett. **78**, 1251 (1997).
  - [3] P. M. Paul, E. S. Toma, P. Breger, G. Mullot, F. Augé, Ph. Balcou, H. G. Muller, and P. Agostini, Science **292**, 1689 (2001).
  - [4] M. Hentschel, R. Kienberger, C. Spielmann, G. A. Reider, N. Milosevic, U. Heinzmann, M. Drescher, and F. Krausz, Nature (London) **414**, 509 (2001).
  - [5] P. B. Corkum and F. Krausz, Nat. Phys. **3**, 381 (2007).
  - [6] P. Salières, A. Maquet, S. Haessler, J. Caillat, and R. Taïeb, Rep. Prog. Phys. **75**, 062401 (2012).

- [7] S. Baker, J. S. Robinson, C. A. Haworth, H. Teng, R. A. Smith, C. C. Chirila, M. Lein, J.W. G. Tisch, and J. P. Marangos, *Science* **312**, 424 (2006).
- [8] P. B. Corkum, *Phys. Rev. Lett.* **71**, 1994 (1993).
- [9] K. J. Schafer, B. Yang, L. F. DiMauro, and K. C. Kulander, *Phys. Rev. Lett.* **70**, 1599 (1993).
- [10] M. Lewenstein, P. Balcou, M. Y. Ivanov, A. LHuillier, and P. B. Corkum, *Phys. Rev. A* **49**, 2117 (1994).
- [11] W. Becker, F. Grasbon, R. Kopold, D. Milošević, G. Paulus, and H. Walther, *Adv. Atom. Mol. Opt. Phys.* **48**, 35 (2002).
- [12] P. Salieres, B. Carre, L. Le Deroff, F. Grasbon, G. G. Paulus, H. Walther, R. Kopold, W. Becker, D. B. Milosevic, A. Sanpera, et al., *Science* **292**, 902 (2001).
- [13] G. Sansone, C. Vozzi, S. Stagira, and M. Nisoli, *Phys. Rev. A* **70**, 013411 (2004).
- [14] C. D. Lin, A.-T. Le, Z. Chen, T. Morishita, and R. Lucchese, *Journal of Physics B* **43**, 122001 (2010).
- [15] T. Morishita, A.-T. Le, Z. Chen, and C. D. Lin, *Phys. Rev. Lett.* **100**, 013903 (2008)
- [16] A.-T. Le, R. R. Lucchese, S. Tonzani, T. Morishita, and C. D. Lin, *Phys. Rev. A* **80**, 013401 (2009).
- [17] M. V. Frolov, A. V. Flegel, N. L. Manakov, and Anthony F. Starace *Phys. Rev. A* **75**, 063407 (2007)
- [18] O. Smirnova, Y. Mairesse, S. Patchkovskii, N. Dudovich, D. Villeneuve, P. Corkum, and M. Y. Ivanov, *Nature* **460**, 972 (2009).
- [19] W. Becker, A. Lohr, M. Kleber, and M. Lewenstein, *Phys. Rev. A* **56**, 645 (1997).
- [20] Lianghui Gao, Xiaofeng Li, Panming Fu, R. R. Freeman, and Dong-Sheng Guo, *Phys. Rev. A* **61**, 063407 (2000)
- [21] J. B. Bertrand, H. J. Wörner, H.-C. Bandulet, É. Bisson, M. Spanner, J.-C. Kieffer, D. M. Villeneuve, and P. B. Corkum, *Phys. Rev. Lett.* **106**, 023001 (2011)
- [22] D. D. Hickstein, *et al.*, *Nat. Photonics* **9**, 743 (2015).
- [23] L. Rego, J. San Román, A. Picór, L. Plaja, and C. Hernández-García, *Phys. Rev. Lett.* **117**, 163202 (2016)
- [24] A. Fleischer, O. Kfir, T. Diskin, P. Sidorenko and O. Cohen, *Nat. Photonics* **8**, 543 (2014).
- [25] P. F. Lan, E. J. Takahashi, K. Midorikawa, *Phys. Rev. A* **81**, 061802(R)(2010).